

## COARSENING OF DECOMPOSED PHASES IN Cu-Ni-Cr ALLOYS

Felipe Hernández-Santiago<sup>1</sup>, Víctor M. Lopez-Hirata<sup>1</sup>, Maribel L. Saucedo-Muñoz<sup>1</sup>, Hector J. Dorantes-Rosales<sup>1</sup>, Jose D. Villegas-Cardenas<sup>2</sup>, Jorge L. Gonzalez-Velazquez<sup>1</sup>

<sup>1</sup>Instituto Politecnico Nacional (ESIQIE);  
Apartado Postal 118-556, Mexico, D.F., 07730, Mexico  
<sup>2</sup>Universidad Politecnica del Valle de Mexico

Keywords: Decomposed phases, Coarsening, Cu-Ni-Cr alloys.

### Abstract

The coarsening process of the decomposed phases was studied in the Cu-34wt.%Ni-4wt.%Cr and Cu-45wt.%Ni-10wt.%Cr alloys aged at 600, 700 and 800 °C for different times by transmission electron microscopy. The morphology of the coherent decomposed Ni-rich phase changed from cuboids to platelets aligned in the <100> Cu-rich matrix directions as aging progressed. The variation of mean equivalent radius of the coherent decomposed phases with aging time followed the modified LSW theory for thermally activated growth in ternary alloy systems. The linear variation of the density number of precipitates and matrix supersaturation with aging time, also confirmed that the coarsening process followed the modified LSW theory in both alloys. The size distributions of precipitates in the Cu-Ni-Cr alloys were broader and more symmetric than that predicted by the LSW theory. The coarsening rate was faster in the symmetrical Cu-45wt.%Ni-10wt.%Cr alloy due to its higher volume fraction of precipitates.

### Introduction

Cu-Ni alloys possess important technological applications because of their good corrosion resistance in sea water and their mechanical properties [1]. The addition of copper to these alloys promotes higher strength even at high temperatures and it also improves their oxidation resistance at high temperatures. Cu-Ni alloys are not suitable for hardening precipitation treatment in spite of the miscibility gap at low temperature [2]. However, the addition of a third alloying element such as Fe, Sn or Cr causes the extension of miscibility gap to higher temperatures. This fact makes possible the precipitation hardening in these alloys because of the enhancement of atomic diffusion at higher temperatures [1,3,4]. Thus, the aging process of a solution treated Cu-Ni-Cr alloy, with composition inside the miscibility gap, causes the decomposition of the supersaturated solid solution into a mix of fcc Cu-rich and Ni-rich phases [5]. The prolonged exposure of Cu-Ni-Cr alloys at high temperatures origins the coarsening or Ostwald ripening of the decomposed phases causing the deterioration of their mechanical properties. The coarsening process of this type of alloys is interesting to be studied because it involves a modulated structure, composed of two coherent Cu-rich and Ni-rich phases. The coarsening process of decomposed phases has been studied by different characterization methods, such as XRD and TEM analyses in the Cu-Ni-Cr alloys [6-8]. Their results reported mainly the evolution of modulation wavelength with aging time based on position measurements of sidebands or satellites in their corresponding patterns. These works pointed out that the change of modulation wavelength with time followed the Lifshitz-Slyozov-Wagner (LSW) theory for a diffusion-controlled coarsening.

Thus, the purpose of present work work is to study the growth kinetics and mechanism of the coarsening process of the decomposed phases in the Cu-34wt.%Ni-4wt.%Cr and Cu-45wt.%Ni-10wt.%Cr alloys aged at 600, 700 and 800 °C for different times using a transmission electron microscope equipped with EDS analysis.

## Experimental Procedure

Cu-34wt.%Ni-4wt.%Cr and Cu-45wt.%Ni-10wt.%Cr alloys were prepared by melting of the pure Cu, Ni and Cr elements with an electrical furnace in an alumina crucible under an argon gas atmosphere. The alloy ingots of 30 mm in diameter and 50 mm in length were encapsulated in a quartz tube under an argon atmosphere, and then homogenized at 950 °C for 10 days. The chemical analysis of both alloys was carried out with Chemical absorption analysis and it showed a good correspondence with the nominal compositions. Specimens of 10 mm x 10 mm x 10 mm were encapsulated in quartz tubes under an argon atmosphere and solution treated at 950 and 1050 °C for 1 h for the Cu-34wt.%Ni-4wt.%Cr and Cu-45wt.%Ni-10wt.%Cr alloys, respectively, and subsequently quenched in ice-water. The solution treated specimens were aged at 600, 700 and 800 °C for 0.6 to 900 ks. The TEM specimens were prepared by the dual jet electropolishing technique with a 33 vol.%HNO<sub>3</sub>-methanol electrolyte at 25 V (DC) and -60 °C and then observed with a TEM equipped with EDS analysis at 200 kV. A beryllium specimen holder was employed for the microanalysis in the aged specimens.

## Results and Discussion

### Morphology of Decomposed Phases

Figures 1 and 2 show the Bright Field (BF)-TEM micrographs of the Cu-34wt.%Ni-4wt.%Cr and Cu-45wt.%Ni-10wt.%Cr alloys aged at 600 °C for different times, respectively. No precipitation was apparent in the as-quenched sample. A modulated structure was observed to occur aligned along the <100> matrix directions, Fig. 1 (a), because of the lower coherent-strain energy associated with these directions [9]. The growth kinetics of spinodal decomposition in the Cu-45wt.%Ni-10wt.%Cr alloy was faster than that in the Cu-34wt.%Ni-4wt.%Cr alloy, after aging. The slow growth kinetics of the latter alloy can be attributed to the smaller driving force for asymmetrical alloys (alloys with compositions close to that of the coherent spinodal line), since the total free energy in the decomposition is much smaller than that in the symmetrical alloy [10]. As aging progressed, the modulated structure was replaced by a periodic tridimensional array of coherent cuboids with planar interfaces parallel to the <100> matrix directions, Figs 1 and 2 (b). Prolonged aging caused a change of morphology from a cuboid array to a platelet-like shape as the cuboids align in rows and coalesce, Figs. 1 and 2 (c). No splitting of precipitates was observed in both the aged alloys. The loss of coherency occurred as evidenced by the appearance of misfit accommodating interfacial dislocations at the interphase interfaces, Fig. 2 (c). At this stage, the morphology of decomposed phase changed to ellipsoidal.

### Coarsening of the decomposed phases

The variation of the mean radius of coherent precipitates with time was fitted by the method of the least squares to the equation of LSW theory [11]:

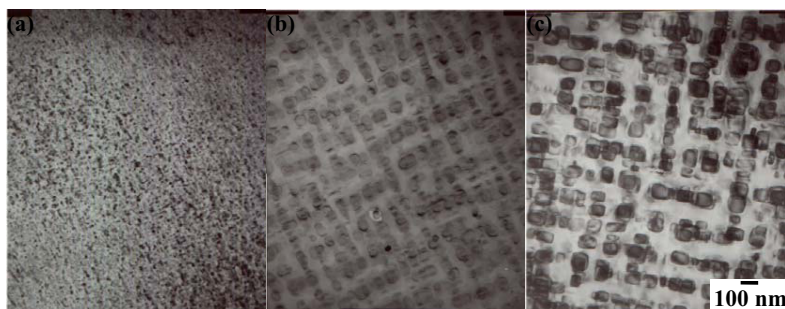


Figure 1. BF-TEM micrographs for the Cu-34wt.%Ni-4wt.%Cr alloy aged at 600 °C for (a) 3.6, (b) 270 and (c) 900 ks.

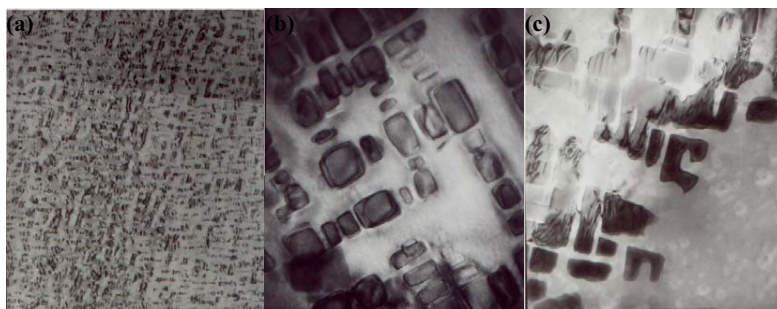


Figure 2. BF-TEM micrographs for the Cu-45wt.%Ni-10wt.%Cr alloy aged at 600 °C for (a) 1.8, (b) 36 and (c) 180 ks.

$$r^3 - r_0^3 = kt \quad (1)$$

where  $r_0$  and  $r$  are the mean radius of precipitates at time  $t = 0$  and time  $t$ , respectively, and  $k$  is a rate constant given by

$$k = 8DV_{\beta}\sigma_{\alpha\beta}/9(c_{\beta}^e - c_{\alpha}^e)G''_{\alpha} \quad (2)$$

where  $D$  is the diffusion coefficient,  $V_{\beta}$  the atomic volume of precipitates,  $\sigma_{\alpha\beta}$  specific interfacial energy of the interface between the  $\alpha$  matrix and  $\beta$  precipitates,  $c_{\beta}^e - c_{\alpha}^e$  the difference between the equilibrium compositions of the  $\beta$  precipitates and  $\alpha$  matrix, and  $G''_{\alpha}$  the second derivative of the molar Helmutz energy of the  $\alpha$  phase.

Figures 3 (a) and (b) shows the straight lines in the plot of  $r^3 - r_0^3$  vs. aging time for the Cu-34wt.%Ni-4wt.%Cr and Cu-45wt.%Ni-10wt.%Cr alloys, respectively. That is, the coarsening process of decomposed phases followed the LSW theory for a diffusion-controlled growth. These figures also showed that the rate constant  $k$ , slope, for the Cu-45wt.%Ni-10wt.%Cr alloy was higher than that for the other alloy composition. It is important to mention that there was a remarkable increase in the rate constant  $k$  for the case of incoherent precipitates in the Cu-34wt.%Ni-4wt.%Cr alloy aged at 800 °C for times longer than 180 ks and in the Cu-45wt.%Ni-

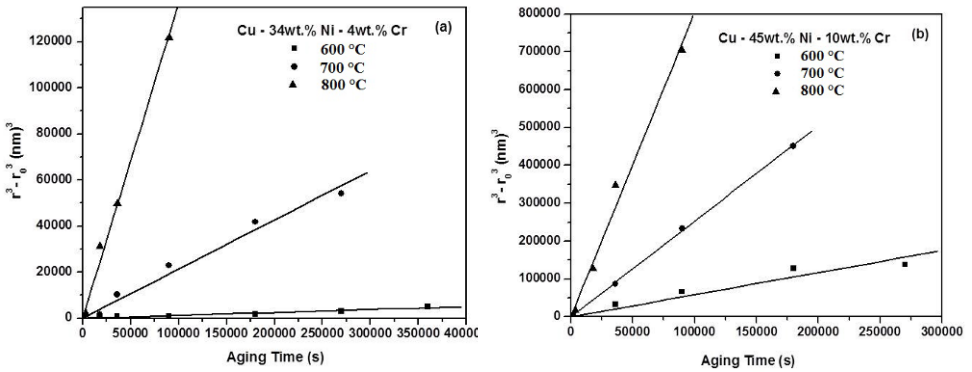


Figure 3. Plot of the cube mean radius of Ni-rich phase vs. aging time for the (a) Cu-34wt.%Ni-4wt.%Cr and (b) Cu-45wt.%Ni-10wt.%Cr alloys.

10wt.%Cr alloy aged at 700 °C for times longer than 270 ks and at 800 °C for times longer than 180 ks, not shown in Figs. 3 (a) and (b).

The temperature dependence of the rate constant  $k$  was expected to follow the Arrhenius relationship. Thus, the activation energy for the coarsening process was determined, from the Arrhenius plot of  $k$ , to be about 182 and 102 kJ mol<sup>-1</sup> for the Cu-34wt.%Ni-4wt.%Cr and Cu-45wt.%Ni-10wt.%Cr alloys, respectively. These values were in agreement with the activation energy 114-254 kJ mol<sup>-1</sup> for the coarsening process determined in Cu-Ni-Cr alloys using the composition wavelength determined from X-ray diffraction analysis [8]. Besides, these values of activation energy are closed to 250-200 and 200-100 kJ mol<sup>-1</sup> corresponding to the interdiffusion process in Cu-Ni and Cu-Cr alloys [12,13], respectively.

This fact confirms that the coarsening of the coherent decomposed phase is controlled by the atomic diffusion in this ternary alloy system.

It has been pointed out [11] that the presence of a non-zero volume fraction of precipitates does not change the exponent of the temporal power law given by the LSW theory, but it changes the scaled distribution functions. Additionally, the rate constant  $k$  increases with the volume fraction of precipitates and the distribution function becomes broader and more symmetric. Thus, the higher volume fraction of precipitates in the aged Cu-45wt.%Ni-10wt.%Cr alloy, compared with that in the other alloy composition, seems to be the possible reason for having higher rate constant values. For example, the volume fractions of precipitate phase were about 0.15 and 0.30 for the Cu-34wt.%Ni-4wt.%Cr and Cu-45wt.%Ni-10wt.%Cr alloys, respectively, aged at 600 °C K for 180 ks. The increase in the rate constant with the volume fraction has been attributed to the increase in the rate of growth and shrinkage of particles because shrinking particles move closer to growing particles [11]. This explanation can be also adopted as the reason for a lower energy activation for the coarsening process in the aged Cu-45wt.%Ni-10wt.%Cr alloy.

The size distributions of the coherent Ni-rich phase in the Cu-34wt.%Ni-4wt.%Cr and Cu-45wt.%Ni-10wt.%Cr alloys aged at 600 °C K for 180 ks are shown in Figs. 4 (a) and (b), respectively. As expected, the size distributions were broader and more symmetric than that predicted by the LSW theory [11]. The size distribution in the Cu-45wt.%Ni-10wt.%Cr alloy, with a precipitate volume fraction of about 0.3, was broader than that in the other alloy composition with a volume fraction of about 0.15.

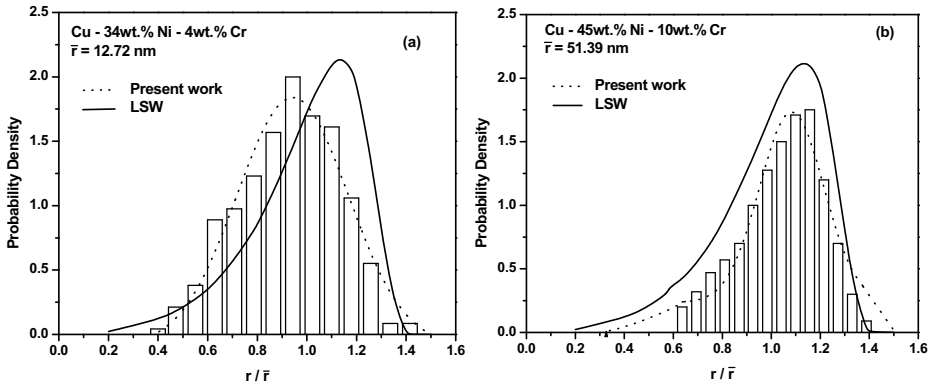


Figure 4. Particle size distribution for the (a) Cu-34wt.%Ni-4wt.%Cr and (b) Cu-45wt.%Ni-10wt.%Cr alloys, after aging at 600 °C for 180 ks.

The plots of the area density number of precipitates  $N_A$  as a function of aging time, expressed as  $t^{-1}$ , in the Cu-34wt.%Ni-4wt.%Cr and Cu-45wt.%Ni-10wt.%Cr alloys aged at 600 °C are shown in Figs. 5 (a) and (b), respectively.  $N_A$  is proportional to the volume density number  $N_V$ . Thus, there is a linear relationship between the number density and time, which confirms that the coarsening process follows the following equation, predicted by the LSW theory [11]:

$$N_V = k_N t^{-1} \quad (3)$$

where the rate constant  $k_N$  is given by

$$k_N = 3f_p/4\pi k f_3 \quad (4)$$

where  $f_p$  is the volume fraction of precipitates and  $f_3$  the third moment of the time-independent scaled particle radius distribution function.

The TEM-EDS microanalysis enabled us to follow the chemical composition of the decomposed phases. Figures 6 (a and b) show, for instance, the Cu and Cr composition, respectively, of the Cu-rich matrix as a function of aging time for the Cu-45wt.%Ni-10wt.%Cr alloy, after aging at 800 °C. At short aging times, the matrix phase became a Cu-rich phase because of the spinodal decomposition process. As the aging progressed the matrix Cu content increased slightly with aging time, while the Ni and Cr contents decreased slightly with aging time. The chemical composition of the decomposed phases, after a prolonged aging in both alloys at 800 °C, is shown in Table I. These values are in a good agreement with the expected values deduced from the miscibility gap of the equilibrium Cu-Ni-Cr diagram at 930 °C [8].

The LSW theory also predicts that the matrix supersaturation  $\Delta c$  decreases with time according to the following temporal power law [11]:

$$\Delta c = k_C t^{-1/3} \quad (5)$$

where the rate constant  $k_C$  is given by

$$k_C = 9(c_\beta^e - c_\alpha^e) k^{2/3}/4D \quad (6)$$

Figures 7 (a) and (b) show the plots of  $\Delta c$  vs.  $t^{-1/3}$  for the Cu-34wt.%Ni-4wt.%Cr and Cu-45wt.%Ni-10wt.%Cr alloys, respectively.  $\Delta c$  was determined by measuring the matrix Cu-rich phase composition for the three chemical elements as a function of aging time and using the following equation:

$$\Delta c = c(\infty) - c(t) \quad (7)$$

where  $c(\infty)$  and  $c(t)$  are the equilibrium composition and that at time  $t$ , respectively. The value of  $\Delta c$  for copper was positive and those for nickel and chromium were negative. This indicated that the matrix phase became richer in copper and poorer in nickel and chromium, as expected in a spinodally decomposed alloy [10]. The data of these plots were fitted to a straight line, which reconfirmed that the coarsening process of the decomposed phases followed the LSW theory for a diffusion-controlled growth in the Cu-Ni-Cr alloys.

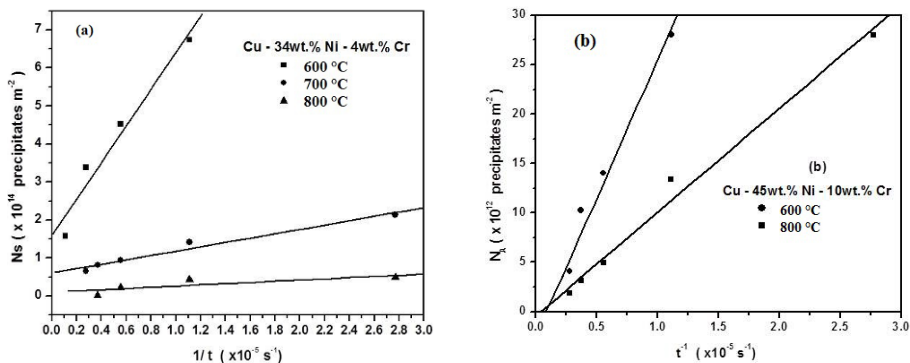


Figure 5. Density number of precipitates versus  $t^{-1}$  for the (a) Cu-34wt.%Ni-4wt.%Cr And (b) Cu-45wt.%Ni-10wt.%Cr alloys.

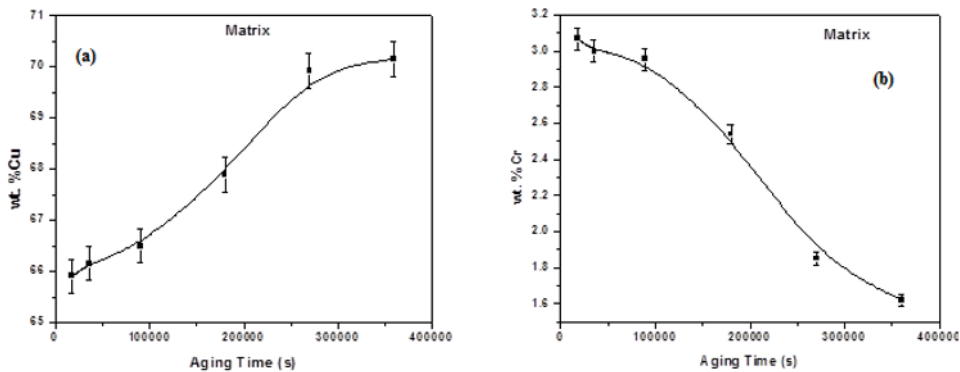


Figure 6. EDS analysis (a) Cu and (b) Cr of the matrix phase for the Cu-45wt.%Ni-10wt.%Cr alloys, after aging at 800 °C.

Table I. Composition (wt.%) of the decomposed phases at 1073 K.

Alloy	Ni-rich Ni-Cu-Cr	Cu-rich Cu-Ni-Cr
Cu-34wt.%Ni-4wt.%Cr	59.0%Ni-25.9%Cu-15.1%Cr	69.5%Cu-28.7%Ni-1.8%Cr
Cu-45wt.%Ni-10wt.%Cr	63.6%Ni-18.0%Cu-18.4%Cr	69.9%Cu-28.2%Ni-1.9%Cr

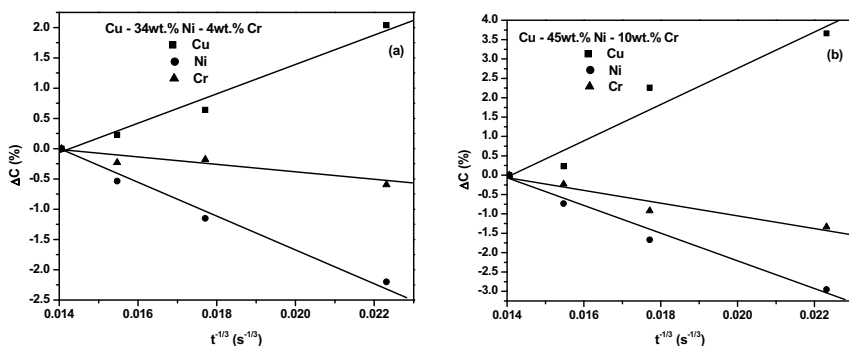


Figure 7. Plot of  $\Delta c$  vs.  $t^{-1/3}$  for the (a) Cu-34wt.%Ni-4wt.%Cr and (b) Cu-45wt.%Ni-10wt.%Cr alloys, after aging at 800 °C.

Kuehmann and Voorhees [14] developed a theory of coarsening in an isothermally aged ternary alloy and they found the exponents of the temporal power laws for the average particle radius, density number, and the matrix supersaturations are the same as that found in the binary system. This is in agreement with the results of this work, shown above. Besides, they also pointed out that the trajectory of the matrix supersaturation lies along a tie-line, but the trajectory of the particle composition does not. In this work, the trajectories of both matrix and particle compositions followed a straight line. However, it is not possible to state whether the slope of the former one corresponds to that of the tie-line because there is no isothermal section for the Cu-Ni-Cr phase diagram at 800 °C reported in the literature.

### Conclusions

A study of the coarsening kinetics of decomposed phases in the Cu-34wt.%Ni-4wt.%Cr and Cu-45wt.%Ni-10wt.%Cr alloys was carried out and conclusions were summarized as follows:

1. The coarsening stage for both alloys followed the three temporal equations for LSW theory for thermally activated growth, with an activation energy of 182 and 102 kJ mol<sup>-1</sup> for the Cu-34wt.%Ni-4wt.%Cr and Cu-45wt.%Ni-10wt.%Cr alloys, respectively.
2. The coarsening rate was faster in the Cu-45wt.%Ni-10wt.%Cr alloy, symmetrical alloy, due to its higher volume fraction of precipitates.
3. The size distributions of particles in the Cu-Ni-Cr alloys were broader and more symmetric than that predicted by the LSW theory.
4. The morphology of the coherent decomposed Ni-Cu-Cr phase changed from coherent cuboids to platelets aligned on the  $\langle 100 \rangle$  directions and subsequently to incoherent ellipsoids.

### Acknowledgements

The authors wish to thank the financial support from SIP-COFAA-IPN and CONACYT.

### References

1. A. Chou, A. Datta, G. H. Meier and W. A. Soffa, *J. Mater. Sci.* **13** (1978)541.
2. H. Baker, *Alloy Phase Diagrams*, vol. 3. (ASM International, Materials Park OH, USA, 1993) p. 173.
3. V. M. Lopez, N. Sano, T.Sakurai and K. Hirano, *Acta metall mater* **41**(1993) 265.
4. L. H. Schwartz, S. Mahajan and J. T. Plewers, *Acta metall* **22** (1974) 601.
5. J. L. Meijering, *Acta metall* **5** (1957) 257.
6. R. I. Saunderson and P. Wilkes, *Acta metall* **26** (1978) 1357.
7. D. Bower, G. W. Lorimer, I. Saunderson and P. Wilkes, *Metals Technology* **7** (1980) 7 120.
8. F. Findik and H. M. Flower, *Mater. Sci. Tech.* **8** (1992)8197.
9. R. J. Livak and G. Tomas, *Acta metall* **19** (1971) 497.
10. H. L. Aaronson, *Phase Transformations* (ASM International, Metals Park OH, USA, 1970) p. 497.
11. G. Kostorz: *Phase Transformations in Materials* (Wiley-VCH, Germany,2001) p. 309.
12. K. Monma, H. Suto and H. Oikawa, *Bull. Japan Inst. Metals* **4** (1984) 4.
13. G. Li, B. G. Thomas and J. F. Stubbins, *Met. Mater. Trans.* **31A** (2000) 2491
14. C. J. Kuehmann and P. W. Vorhees, *Met. Mater. Trans.* **27A** (1996) 937.